Evaluation of Cooperative Spectrum Sensing based on Large Scale Measurements

Matthias Wellens, Janne Riihijärvi, Martin Gordziel and Petri Mähönen
Department of Wireless Networks, RWTH Aachen University
Kackertstrasse 9, D-52072 Aachen, Germany
email: {mwe, jar, mgo, pma}@mobnets.rwth-aachen.de

***Abstract*—Dynamic spectrum access to unused licensed spectrum has been proposed as solution to the spectrum scarcity problem. Reliable detection of any primary user signal is crucial for the required interference-free operation. It has been shown that cooperative sensing has the potential to alleviate propagation effects such as fast fading or shadowing and thus to improve sensing reliability. However, there is lack of practical studies confirming the theoretical results. In this paper we present our measurement setup for cooperative sensing and detailed experimental results that prove the major findings. Cooperative sensing can improve the detection reliability and lower the sensitivity requirements on single sensors. We also validate that correlated spectrum measurements will lower the cooperation gain and that such correlations decrease with distance. Additionally, we develop a metric for the robust representation of these correlations and discuss the impact on practical system design. More precisely, we elaborate on different modelling approaches that cognitive radios may apply in order to learn about their radio environment and to exploit such knowledge for enhanced dynamic spectrum access.**

I. Introduction

The recent success of wireless communication and its services has resulted in an increasing need for radio spectrum. The advent of broadband technologies further accelerates this process. From a regulatory point of view, licenses for numerous services have been issued. Especially, nearly no free frequencies below 3 GHz that have the commercially most interesting propagation characteristics are available. This situation is often referred to as the spectrum scarcity problem [1]. However, several measurements have shown that spectrum usage is rather inefficient [2]–[6] because multiple services are active either only for a fraction of time or in a fraction of the spatial area the license is valid for. This has led to the vision of Dynamic Spectrum Access (DSA) [7], [8].

If the system possessing the license for a spectrum band, often called the primary user, does not use it, secondary users may opportunistically access it in an unlicensed fashion [9]. The underlying requirement for allowing such secondary access is that only strictly limited interference to any primary transmission is caused by the secondary networks. Therefore, the task of identifying unused spectrum bands, usually called spectrum sensing [10], is crucial for efficient performance of any DSA system. Different sensing techniques can be applied depending on the available a priori information on the waveform to be searched for. The most general method is energy detection [11], which applies a threshold to the received power in order to decide on the presence of a primary transmission and does not require any a priori knowledge. If information on pilot signals [12], [13] or periodicities of the sensed signal is available specialized feature detection techniques can improve the performance. In this context, cyclostationary feature detection is the most studied technique exploiting periodicities present in primary user signals [14]–[16]. Finally, matched filter reception will be the optimal detector if complete knowledge of the examined waveform is available [17].

The secondary user may receive the primary signal heavily attenuated or in a deep fade. Such conditions significantly increase the complexity of the sensing task. Cooperative sensing has been proposed as a technique to compensate especially fading and shadowing effects [18]–[20]. However, most of the related studies are purely theoretical and only few experimental results, gathered in an indoor scenario [21], [22], exist on how much corporation gain can be achieved in practice. Additionally, the shadowing experienced by the cooperating secondary users may be correlated but the major existing models describing this phenomenon, e.g. [23], [24], were developed based on measurements in the cellular context with assumptions that are not perfectly accurate for DSA scenarios.

In this paper we present a measurement setup explicitly designed to evaluate spectrum usage over larger areas. Such enhanced methodology is required as a solid basis for reliable, distributed spectrum measurements and as an important step towards practical DSA applications. We focus on the correlation of measurement data taken at different locations and comment on the consequences for future protocol development and system deployment. We discuss the gathered results and show that the major theoretical findings are confirmed also in our practical scenario. We also extend the analysis to more appropriate metrics for describing how similar spectrum measurements are. Using these metrics one can flexibly compare data recorded at different locations.

Additionally, we present approaches how the efficiency of cooperative sensing could be enhanced by exploiting correlated measurement results for efficient distribution of the spectrum sensing task across multiple nodes. In this context, we discuss previous work carried out by the wireless sensor networks community and point out open research problems on the way towards complete systems.

Finally, we discuss different approaches how the spatial

characteristics of spectrum usage could be modelled more realistically. These approaches could also enable cognitive radios (CRs) to enhance their view on the spectrum usage through building up appropriate models at runtime.

The rest of this paper is structured as follows. We start in Section II with a more detailed review of cooperative sensing. We continue in Section III with the description of our measurement setup and the examined scenarios. We introduce the main applied evaluation criteria in Section IV before we show results in Section V. Afterwards, we discuss alternatives for spectrum modelling in Section VI and finally conclude the paper in Section VII.

II. Cooperative sensing

There are several scenarios in which a single secondary user is likely to miss a primary transmission and mistakenly assumes a spectrum band to be free and available for opportunistic use. In such a situation the secondary transmission may cause harmful interference to the primary system. Cooperative sensing has been proposed[1] to cope with some of the problems that result from the mentioned scenarios.

Most notably, there is the well-known hidden node problem in which the secondary user is either too far away from the primary transmitter or the signal is attenuated because of buildings or other obstacles in the propagation path. If the spectrum sensor is more sensitive than any primary receiver, the additional margin can cover possibly higher signal attenuation experienced by the secondary receiver. However, propagation effects cannot always be fully compensated assuming a realistic margin[2]. Instead, cooperation with other secondary users is a more efficient solution. If, for example, one of these users does not suffer from similarly sever shadowing but receives a stronger primary signal, he will detect the transmission and will inform the other secondary nodes not to use this frequency.

Fast fading may cause a severe drop in the received signal power and a missed detection. Cooperative sensing can help to solve this problem because fast fading is only correlated over distances of the order of the used wavelength [25]. More specifically, it has been shown that the additional sensitivity margin required to cope with signal fades caused by multipath propagation approaches asymptotically zero when increasing the number of cooperating users [20]. Thus, the achievable cooperation gain can also be exploited to lower the sensitivity requirements for each single participating node.

The case of shadowing deserves further discussion because shadowing is correlated over longer distances. A simple example is the fact that nearby secondary users may be located behind the same building and thus are both shadowed from the primary transmitter located on the other side of that building. Detailed studies on the characteristics of these correlations have been performed in the context of cellular networks also based on extensive measurement campaigns [23], [24], [26]–[29]. However, these studies have several drawbacks when applied to DSA networks. First, the cellular base station, which resembles the primary user in the DSA context, was under the control of the researchers. Second, usually a single or at maximum two base stations were considered and their locations were known. In the case of DSA, we know neither the number nor the locations of the active primary transmitters[3]. Third, the existing studies were based on cellular systems and thus focused on a small set of frequencies. In contrast, the vision of DSA is not limited to a few frequency bands allowing secondary users to benefit from their extreme frequency agility. These facts motivated our measurement campaign with an explicitly designed measurement setup as described in Section III.

Despite its focus on cellular systems, the model introduced by Gudmundson in [23] has turned out to be very useful also in the context of DSA. It gives the normalized autocorrelation function $\phi(\Delta d)$ as

$$\phi(\Delta d) = e^{\frac{-ln2}{d_{corr}}|\Delta d|}, \tag{1}$$

where Δd is the change in distance and d_{corr} is the decorrelation length ($\phi(d_{corr}) = 0.5$) which depends on the environment. Through fitting of measured data, Gudmundson determined d_{corr} to be 347 m in a suburban environment at 900 MHz and to be 5.76 m in an urban environment at 1700 MHz [23]. The model was found to work satisfactorily for distances up to 500 m in the suburban areas, but only in the range of 10–15 m in the urban environment.

Several researchers used the Gudmondson model in order to calculate the cooperation gain under spatially correlated shadowing. It was shown that correlation of the shadowing experienced by multiple secondary users lowers the cooperation gain, see, e.g., [18]–[20]. Additionally, Ghasemi and Sousa showed that the cooperation gain will be maximized if the cooperative users are located as far away from each other as possible. Such locations will ensure the least correlated measurements and will lower the reduction in cooperation gain [30]. Following a similar rationale, Mishra *et al.* [20] showed that the cooperation gain is limited by the cooperation footprint, which corresponds at maximum to the primary transmitter's coverage.

Various research groups investigated further aspects of cooperative sensing. Especially, the question how the data fusion of the measurement results should be performed gained interest. Taherpour *et al.* have studied the aspect of exchanging quantized measurement results instead of binary detection decisions in [31]. More advanced fusion rules than the simple *OR*-rule have been investigated and shown to perform better in [32].

[1]Cooperative sensing could be implemented in a centralized as well as in a distributed fashion. Since the involved differences are not of importance in our studies we do not consider the underlying system architecture in detail in the remaining paper.

[2]In case of the IEEE 802.22 system this margin is assumed to be 30-50 dB [12].

[3]We assume here the general case that no detailed a priori knowledge on the primary user system is available.

A. Further related work in collaborative processing

We conclude this section by commenting on other efforts in the collaborative sensing domain with potential applications in DSA. Collaborative *localization* has been studied extensively in the wireless networks research community [33]–[35]. Usually, these techniques are RSSI[4] based, applying Bayesian reasoning to ascertain the probability distributions for locations of signal sources based on noisy measurements. Such techniques could be used in the DSA environment to localize primary users, and extended to estimate the needed safety regions around those. For early results on such a scheme in the case of a single transmitting primary user, see [36].

Inferring the *presence* of a primary user is closely related to the distributed sensing problem studied especially in the wireless sensor networking (WSN) community. For an accessible overview, the reader is referred to [37], [38]. Usually, the distributed sensing problem is formulated in terms of local measurements carried out at the collaborative nodes. The gathered data is quantized and exchanged according to the needs of a distributed or centralized protocol for the actual inference. For a discussion of optimal sensor data fusion in general see, e.g., [39], [40]. In addition to a higher reliability of the overall sensing process, another goal is to reduce the sensing load assigned to each participating node. This can be achieved by exploiting the correlations in the measured data and by distributing the sensing task accordingly.

There are, however, some interesting differences between the considered DSA scenario and the traditional WSN case that should be taken into account. The most significant of these is the added scheduling requirement on the sensing process itself. The data transmission is interrupted whenever the spectrum is being sensed outside the currently used band unless a second radio is used for spectrum sensing as suggested, e.g., in [41]. Since the second radio will incur additional energy consumption and increase the complexity of the node, approaches working with a single radio interface are preferable. Thus, there will be a motivation to minimize the total sensing time especially if delay-sensitive applications are being run on the node. The second major difference to the WSN case is the cost of communication. In much of the distributed sensing work it is assumed that only a few bits of measurement information should be exchanged between the nodes to conserve energy, whereas in many foreseen CR applications this requirement can be considerably relaxed. The third difference is the increased heterogeneity in the network in terms of the significance of the measurements made by individual nodes. Especially in an urban environment some of the nodes participating in the sensing process might be indoors or shadowed, significantly reducing their capability of inferring anything about the activities of the primary users.

III. Measurement setup

In the preceding section we discussed cooperative sensing in detail. As mentioned, most of the existing results on cooperative sensing are based on theory and there is lack of larger scale experimental evaluations, especially in outdoor scenarios. Therefore, we developed a new measurement setup starting from our static spectrum occupancy evaluation setup which was presented in [5]. In order to make it especially suitable for cooperative spectrum sensing scenarios a number of new requirements were taken into account.

Fig. 1. Both measurement setups as used during the CeBIT industry fair in Hanover, Germany.

First, we wanted to evaluate cooperative sensing in different frequency bands that are used for different wireless technologies. This flexibility narrows the selection of sensing techniques down to energy detection because it is the only method that does not rely on any a priori knowledge of the primary user technology. Second, since other detection techniques usually outperform energy detection (see, e.g., [22]) we needed a very sensitive energy detection setup in order to ensure useful results. Third, supervising multiple cooperative spectrum sensors is impractical because of the equipment and personal costs. Instead, we decided to use only two setups and investigate multiple locations one after another. In order to guarantee that both setups evaluate the same frequency in parallel, both setups had to be time-synchronized with high precision. Fourth, the setup had to be waterproof for outdoor operation. Since we planned to examine multiple locations, each setup had to be mobile and able to operate autonomously without access to power supply or wireless communication capabilities.

In order to fulfill these requirements we selected portable Rohde & Schwarz FSL6 spectrum analyzers with inbuilt preamplifiers[5] as basis for our two identical setups. We enabled DC supply for the instruments and added absorbent glass mat (AGM) leadacid accumulators in order to allow for the autonomous operation throughout a full day. We used ruggedized laptops for the instrument control via Ethernet and for data saving purposes. The software is based on the instrument

[4]Received Signal Strength Indicator

[5]The typical displayed average noise level (DANL) at 1 GHz is -160 dBm (1 Hz) using the inbuilt preamplifier [42].

TABLE I
SPECTRUM ANALYZER CONFIGURATION USED THROUGHOUT THE MEASUREMENTS

Band 1: 370-570 MHz	TETRA, DVB-T, analog TV
Band 2: 800-1000 MHz	GSM, DVB-T
Band 3: 1720-1820 MHz	GSM1800, DECT
Band 4: 1920-2170 MHz	UMTS, span = 250 MHz
Band 5: 2350-2550 MHz	WLAN, BT
Frequency span	200 MHz
Resolution bandwidth	100 kHz
Number of measurement points	2001
Sweep time	250 ms
Detector type	Average detector

control toolbox of the MATLAB software package, appropriate instrument drivers, and significant bespoke extensions. All hardware components were enclosed in a wooden weatherproof box and installed onto a carriage to enable mobility. We used the same antennas as successfully tested in our previous stationary measurement campaign [5]. We covered the frequency range from 20 MHz to 3 GHz with two discone antennas of different sizes. Both are vertically polarized, nearly omnidirectional in the horizontal plane and slightly directed in the vertical plane. Figure 1 shows both measurement setups next to each other[6].

We achieved time-synchronization using the Global Positioning System (GPS). We deployed Garmin GPS18 LVC receivers and fed their pulse-per-second signals to the external trigger inputs of the spectrum analyzers. We configured the sweep time to be 250 ms, which is the exact time spent for measurements. However, the time spent when switching from one frequency to the next one is not fixed and may vary depending on other operations run in parallel by the multitasking capable operating systems of the instruments. In order to limit the impact of these operations, that may cause loss of synchronization, we selected a span of 200 MHz and 2001 measurement points after extensive testing. The resolution bandwidth was configured to 100 kHz accordingly. Finally, we used an average detector in order to limit the noise variance. All settings are summarized in Table I including the selected spectrum bands and the most popular services for each band.

We evaluate only two locations in parallel although cooperative sensing systems will probably consist of more nodes. We assume that the data gathered at different locations and different times is comparable[7]. In this context we define *spectrum occupancy* $\Omega(t, f)$ at sample index t and frequency index f as follows. We applied energy detection and used the detection threshold γ:

$$\Omega(t,f) = \begin{cases} 0 & \text{if } P_{rx}(t,f) < \gamma \\ 1 & \text{if } P_{rx}(t,f) \geq \gamma \end{cases}, \tag{2}$$

where $P_{rx}(t, f)$ is the received power. If $\Omega(t, f) = 1$ the measured channel will be counted as *occupied*, samples with a received power below γ indicate a *free* channel, respectively. Furthermore, let us denote by N_s the number of measured samples and by DC_f the duty cycle computed for frequency channel f, given by

$$DC_f = \frac{1}{N_s} \sum_{t=1}^{N_s} \Omega(t,f). \tag{3}$$

Usually, DC is given in percentage and this is the convention observed in the tables and figures in this paper as well.

We evaluated the DC averaged over complete bands considering only those channels that exhibit a $DC > 0$. Examples for such bands are the whole ISM[8]-band at 2.4 GHz or the whole UMTS[9] uplink (UL) band. The changes in DC throughout our measurement time (around 8:30 in the morning to around 17:30 in the afternoon) were rather small and were generally in the order of 5-8 % for all tested services. We could determine the change over time because we moved only one setup and kept the other one stationary at a single location as a reference system. More drastic changes could be observed when investigating single channels but the averaging over whole bands allows us to reasonably compare and combine results taken at different locations and times.

In contrast, certain characteristics of the deployed technologies have significant impact on the results. The transmit power, the spatial transmitter distribution, and the medium access control are the most important of these properties. The former two are straightforward because they have direct impact on the area covered by the primary service, which in our case are all licensed legacy services. The latter one also leads to distinct differences. CDMA[10]-based technologies such as UMTS transmit continuous signals in the downlink (DL) direction even if only control channels are in use. Therefore, the determined DC is usually be very high. The DC of TDMA[11]- or CSMA[12]-based technologies varies dynamically and depends on the network load.

A. Measurement scenarios

We performed our measurements in three different scenarios. First, we had the opportunity to measure at the CeBIT industry fair in March 2008 in Hanover, Germany. Additionally, we run two campaigns in the city of Aachen, Germany, also in March 2008. Each campaign took approximately eight to nine hours.

The CeBIT industry fair is certainly not a typical example but it represents an extreme case in terms of the usage of wireless services and the density of users. However, even in such a scenario a significant amount of unused spectrum could be found. In parallel, a very high usage of the most popular systems, such as GSM or WLANs, could be observed.

[6]The photograph also shows a radom antenna which we used to investigate frequencies above 3 GHz. Since only few popular services work on such high frequencies we do not present these results here.

[7]Technically, this means we assume a suitable stationarity property of the underlying process.

[8]Industrial, Scientific, and Medical.

[9]Universal Mobile Telecommunications System.

[10]Code Division Multiple Access.

[11]Time Division Multiple Access.

[12]Carrier Sense Multiple Access.

We focused most of our measurements on the ISM-band at 2.4 GHz where WLAN stations were the dominating type of transmitters. We performed these measurements indoors in the connected halls 14 and 15 because of the installed GPS-repeaters that enabled live demonstration of new navigation devices. We used these signals for synchronization of our setups. We placed one setup, in the following called the stationary, at a central location in hall 15 and moved the other setup, the mobile one, throughout the halls 14, 15, and parts of 16. We covered an almost regular grid with 70 points and a step size of $\approx$12.5 m. We gathered 200 samples per location, meaning that we took 200 sweeps before moving the mobile setup to the next grid point and starting the next measurement.

We applied a similar grid in both other scenarios in the downtown area of Aachen. For short range services such as WLAN or DECT, we selected 60 locations with a step size of $\approx$15 m. For mid-range services such as GSM or UMTS we selected 52 locations with a coarser step size of $\approx$250 m. These distances were compromises between the number of different locations and the overall covered area. The latter is strictly related to the number of primary transmitters deployed in the area. In order to limit the measurement time we lowered the number of samples taken at each location to 150. Prior tests showed that sufficient statistics could still be computed.

IV. Evaluation criteria

Following the initial definition by Joe Mitola [43], cognitive radios (CRs) will be aware of their environment. For our special case this means that CRs that participate in cooperative sensing would need to learn about the correlation properties of spectrum measurements taken by different secondary users. Such approaches have already been published in the context of radio environment maps [44], [45]. CRs could exploit such knowledge in order to optimize which secondary user senses which spectrum band at which time. In this section, we present metrics that could be used to describe correlation characteristics starting from the differences to classical shadowing correlation models.

The most popular of these models, e.g. [23], are based on shadowing correlation measurements performed in the cellular context. Appropriate preprocessing was applied to the gathered data, in detail, the impact of signal attenuation over distance and multipath propagation were eliminated in order to extract only the shadowing process. Since the location of the transmitter andthe attenuation exponent were known, the major signal attenuation effect could almost be compensated. Additionally, multiple measurements at locations only a few wavelengths away from each other were taken and averaged in order to nearly eliminate the impact of multipath propagation as well. The former step requires knowledge of the location of the primary transmitter and the surrounding environment which is usually not available in the DSA case. Therefore, extracting only the impact of shadowing correlation cannot be achieved by any secondary user without detailed a priori knowledge of the primary system. Although inferring the primary transmitter location on-line may be feasible, measuring the path loss is much more complex without knowledge of the primary transmission power.

Instead, we can only model the correlations of the received power measured by different secondary users. If not only energy detection is applied the strength of single features or other signal characteristics could also be modelled. Since we do not consider feature detection in this paper we will focus on the received power. In the following, we will discuss different metrics that could be used to evaluate the similarity of the received power measured by two secondary users[13].

A. Correlation metrics

The cross-correlation $R(\mathbf{U}, \mathbf{V})$ between two independent processes is defined as

$$R(\mathbf{U}, \mathbf{V}) = \frac{1}{N_s} \sum_{t=1}^{N_s} U_t \cdot V_t, \tag{4}$$

where N_s is the number of samples, $\mathbf{U}$ and $\mathbf{V}$ are the vectors to be compared, and U_t and V_t are their components, respectively. In our case $\mathbf{U}$ and $\mathbf{V}$ correspond to the time series of the received power measured synchronously by two secondary users.

The main drawback of the bare cross-correlation is its dependence on the absolute received power and the duty cycle. If the duty cycle at the evaluated frequency is high the cross-correlation will be high as well. Similarly, if a strong primary user signal is received also the cross-correlation will be high. However, both characteristics do not mean that the measurements taken by the two secondary users are very similar.

B. Covariance

The dependence on the absolute power can be compensated in some cases by subtracting the average received power. The resulting covariance $\mathrm{cov}(\mathbf{U}, \mathbf{V})$ is computed as

$$\mathrm{cov}(\mathbf{U}, \mathbf{V}) = \frac{1}{N_s} \sum_{t=1}^{N_s} (U_t - \overline{\mathbf{U}}) \cdot (V_t - \overline{\mathbf{V}}), \tag{5}$$

where $\overline{\mathbf{U}}$ and $\overline{\mathbf{V}}$ denote the average power received by the two secondary users. Additionally, the covariance $\mathrm{cov}(\cdot)$ is often extended by normalization[14]:

$$\rho(\mathbf{U}, \mathbf{V}) = \frac{1}{N_s} \sum_{t=1}^{N_s} \frac{U_t - \overline{\mathbf{U}}}{\sigma_{\mathbf{U}}} \cdot \frac{V_t - \overline{\mathbf{V}}}{\sigma_{\mathbf{V}}}, \tag{6}$$

where $\sigma_{\mathbf{U}}$ and $\sigma_{\mathbf{V}}$ are the standard deviations of the received power vectors.

[13] Due to the lack of reference information on the primary user activity in our measurement scenarios we will not consider the performance metrics probability of missed detection or probability of false alarm, that are very popular in the DSA context.

[14] In the communication, statistics, and time series communities partially different definitions for the terms correlation, covariance, correlation coefficient, etc. are used. No common formulations can be found. Therefore, we included complete mathematical definitions in order to avoid confusion as much as possible. Additionally, the terms *similarity* and *correlation* are used interchangeably throughout the remaining paper.

TABLE II
COMBINATIONS OF DETECTION EVENTS AT THE STATIONARY AS WELL AS THE MOBILE SPECTRUM ANALYZER (SA).

Elementary detection events	Detection at mobile SA $\Omega_{mob}(t,f)$	Detection at stationary SA $\Omega_{sta}(t,f)$
NO	0	0
AND	1	1
EX_{mob}	1	0
EX_{sta}	0	1

Combined detection events	Corresponding set of elementary events
XOR	EX_{mob} + EX_{sta}
OR	*AND* + EX_{mob} + EX_{sta}

The $\mathrm{cov}(\cdot)$ is independent of the absolute value of the evaluated vectors because of the correction by the mean. However, this is not always desirable. A base station in a CDMA-based UMTS network will at minimum constantly use the broadcast channel, transmit a continuous signal, and announce its presence to new client devices trying to join the network. Additionally, no feedback is available for such common channels and significantly less transmit power adaptations are conducted by the base stations. Resulting from these facts the measured received power shows noise-like behaviour over time although on a significantly higher power level. However, the correction by the mean applied during the calculation of the covariance metric would filter out the higher power level and a UMTS signal would look like noise. Thus, also the covariance is suboptimal for our case.

C. Binary correlation metrics

Before introducing a new metric which is not susceptible to the effects discussed for the cross-correlation and the normalized covariance, we reconsider our system at hand. In a DSA scenario, we are solely interested in the binary decision if the primary user is present or not. Although it has been shown that soft-decision making may perform better in some situations [18], [31], we start from a simple *OR*-fusion of local binary decisions.

We consider a simple two node secondary network as represented by our measurement setup. In this case, those samples that led to the detection of the primary at both nodes or none of them do not provide additional information through cooperation. Instead, those samples that were detected only by a single spectrum analyzer represent the cooperation gain. Following this line of thought, Table II lists the most important detection events.

Next, we compute the probability of each event throughout the time the mobile SA was placed at one location[15]. We define the *AND*-ratio for frequency index f as

$$\begin{aligned}\alpha(f) &= \frac{1}{N_s}\sum_{t=1}^{N_s} \Omega_{mob}(t,f) \ \wedge \ \Omega_{sta}(t,f) \\ &= \frac{1}{N_s}\sum_{t=1}^{N_s} AND_{mob,sta}(t,f),\end{aligned} \tag{7}$$

where $\Omega_{sta}(t,f)$ is the spectrum occupancy detected by the stationary SA and $\Omega_{mob}(t,f)$ the one determined by the mobile SA, respectively. The constant N_s is the number of samples taken at the investigated location. Similarly, we define the *XOR*-ratio as

$$\begin{aligned}\xi(f) &= \frac{1}{N_s}\sum_{t=1}^{N_s} \Omega_{mob}(t,f) \ \oplus \ \Omega_{sta}(t,f) \\ &= \frac{1}{N_s}\sum_{t=1}^{N_s} XOR_{mob,sta}(t,f).\end{aligned} \tag{8}$$

The ratios $\alpha(f)$ and $\xi(f)$ describe the probability that a sample is either detected by both SAs or by only one of them. A high value for $\alpha(f)$ indicates that cooperation would not improve sensing significantly because most samples were detected by both nodes. A high value for $\xi(f)$, however, describes the situation with multiple samples that were detected by a single node and, thus, situations where cooperation would improve the sensing reliability at the other node.

In order to be less dependent on the characteristics of a single measurement channel we average over all channels N_f belonging to the same spectrum band or service[16]. If we assume that the spectrum band we are interested in starts with channel index F the averaged *AND*- and *OR*-metrics become

$$\alpha_{service} = \frac{1}{N_f}\sum_{f=F}^{F-1+N_f} \alpha(f), \tag{9}$$

$$\xi_{service} = \frac{1}{N_f}\sum_{f=F}^{F-1+N_f} \xi(f). \tag{10}$$

In order to quantify which node benefits more from cooperation we define two more ratios:

$$\begin{aligned}\beta_{sta,service} &= \frac{1}{N_f}\sum_{f=F}^{F-1+N_f} \frac{\sum_{t=1}^{N_s} \neg\Omega_{mob}(t,f) \ \wedge \ \Omega_{sta}(t,f)}{\sum_{t=1}^{N_s} \Omega_{mob}(t,f) \ \vee \ \Omega_{sta}(t,f)} \\ &= \frac{1}{N_f}\sum_{f=F}^{F-1+N_f} \frac{\sum_{t=1}^{N_s} EX_{sta}(t,f)}{\sum_{t=1}^{N_s} OR_{mob,sta}(t,f)},\end{aligned} \tag{11}$$

[15]All metrics and ratios introduced in the following are specific to a pair of measurement locations. More precisely, they are specific to the location of the mobile SA since we did not move the stationary SA throughout one campaign. Thus, we will omit the spatial dependence on the coordinates x and y, e.g., $\Omega(x,y,t,f) = \Omega(t,f)$, for clarity.

[16]In real systems cooperative users will have to evaluate the correlation on a per channel basis if different primary transmitters use these channels. However, since the DC changes of a single channel are significantly larger compared to whole bands we average over whole bands in order to lower the impact of the DC. Additionally, this step enables us to provide more generally applicable results.

$$\beta_{mob,service} = \frac{1}{N_f} \sum_{f=F}^{F-1+N_f} \frac{\sum_{t=1}^{N_s} \Omega_{mob}(t,f) \ \wedge \ \neg\Omega_{sta}(t,f)}{\sum_{t=1}^{N_s} \Omega_{mob}(t,f) \ \vee \ \Omega_{sta}(t,f)}$$
$$= \frac{1}{N_f} \sum_{f=F}^{F-1+N_f} \frac{\sum_{t=1}^{N_s} EX_{mob}(t,f)}{\sum_{t=1}^{N_s} OR_{mob,sta}(t,f)}. \quad (12)$$

The metric $\beta_{sta,service}$ gives the probability that the mobile SA could get new information from the stationary SA and $\beta_{mob,service}$ denotes how probable it is that the mobile SA could provide new information to the stationary one. For instance, if the mobile is positioned much closer to the primary transmitter a high value for $\beta_{mob,service}$ is to be expected because the stationary will receive a weaker primary user signal.

D. Weighted correlation metric

The above ratios consider solely the binary energy detection result. Therefore, the information if both nodes received a similarly strong signal or one of them got a weaker signal will not be considered although the absolute power has significant impact on how similar the measurement results are. The above ratios are also susceptible to different detection thresholds or varying primary system duty cycles.

For example, if the received power at both cooperative nodes is very close but the detection threshold is exactly in between, the binary energy detection will falsely indicate that the nodes' measurement results are not similar. In the next step we correct this behaviour and consider the difference $\Delta P_{rx}(t,f)$ in received power measured at both nodes:

$$\Delta P_{rx}(t,f) = P_{rx,sta}(t,f) - P_{rx,mob}(t,f). \quad (13)$$

We aim at the following behaviour for our correlation metric, that we introduce in this section: If $\Delta P_{rx}(t,f)$ is very large and both measurements trigger detections, the specific *AND*-event should contribute less to the similarity-metric compared to the case with small $\Delta P_{rx}(t,f)$. If $\Delta P_{rx}(t,f)$ is small but only one of the measurements triggers a detection, the specific *XOR*-event should lower the similarity metric much less compared to the case of large $\Delta P_{rx}(t,f)$ and only one detection.

In order to implement the described behaviour we apply exponential weighting functions to each *AND*- and *XOR*-event by defining

$$\omega_{AND}\big(\Delta P_{rx}(t,f)\big) = \exp\left[-\frac{1}{2}\left(\frac{10\log_{10}(\Delta P_{rx}(t,f))}{10\log_{10}(c_{AND})}\right)^2\right], \quad (14)$$

and

$$\omega_{XOR}\big(\Delta P_{rx}(t,f)\big) = 1 - \exp\left[-\frac{1}{2}\left(\frac{10\log_{10}(\Delta P_{rx}(t,f))}{10\log_{10}(c_{XOR})}\right)^2\right]. \quad (15)$$

Figure 2 shows both weighting functions plotted over $\Delta P_{rx}(t,f)$. The normalization constants c_{AND} and c_{XOR} were chosen in order to realize the goals explained at the beginning of this section.

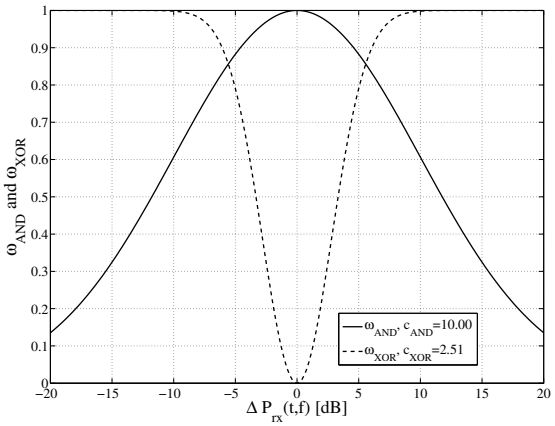

Fig. 2. Weighting functions as used to consider the difference in received power measured at two cooperative secondary users.

Finally, we combine $\alpha(f)$ and $\xi(f)$ in order to describe the similarity of the power measurements performed by two cooperative nodes in a single weighted metric. As discussed above, *AND*-events represent the correlation in our scenarios and the higher the probability of these *AND*-events is the higher should be the correlation metric.

Applying the discussed weights to a combination of the binary metrics results in such behaviour and gives the weighted *AND-OR* metric

$$\Phi(f) = \frac{\sum_{t=1}^{N_s} \omega_{AND} \cdot AND_{mob,sta}(t,f)}{\sum_{t=1}^{N_s} AND_{mob,sta}(t,f) + \omega_{XOR} \cdot XOR_{mob,sta}(t,f)}. \quad (16)$$

The denominator of equation (16) corresponds to a weighted *OR* because it uses the sum of *AND* and *XOR*, which is equal to the combined detection event *OR* (see Table II).

Similarly as above we can now also average $\Phi(f)$ over a whole spectrum band to obtain the service-specific metric

$$\Phi_{service} = \frac{1}{N_f} \sum_{f=F}^{F-1+N_f} \Phi(f). \quad (17)$$

V. Results

After describing different metrics for assessing the similarity of spectrum measurements at two nodes we shall now present selected results based on our extensive measurement campaign.

A. Binary detection metrics

We will start with the simple case discussed in Section IV-C, where binary hard decisions are exchanged between secondary users. Figure 3 shows a summary of our ISM-band measurements carried out at the CeBIT industry fair and in downtown Aachen. All samples were grouped into distance bins and the probabilities $\alpha_{service}$ and $\xi_{service}$ were determined using

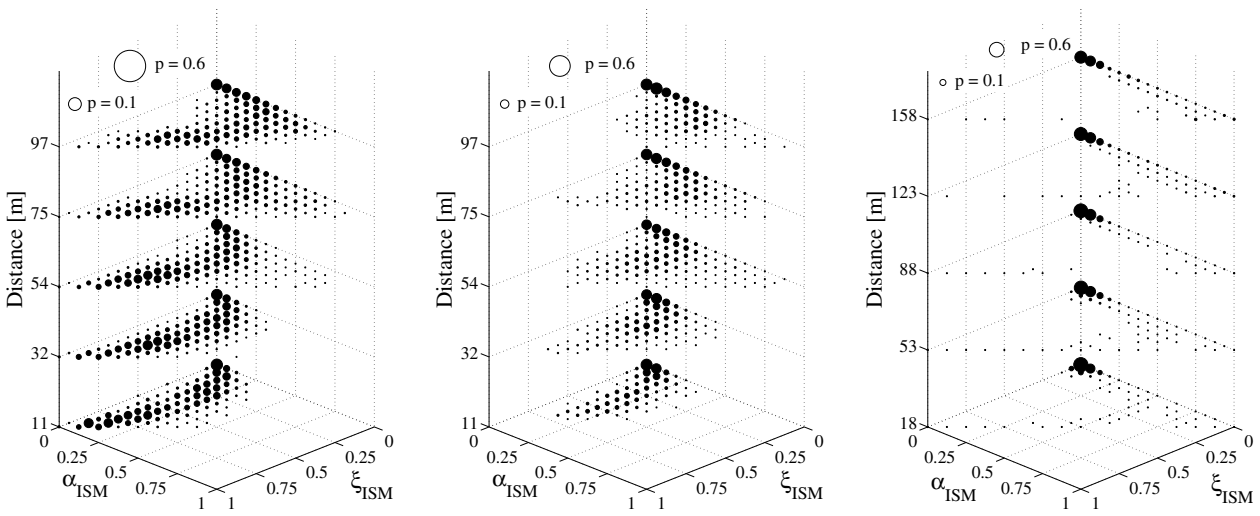

(a) CeBIT hall, detection threshold γ=-101 dBm.

(b) CeBIT hall, γ=-91 dBm.

(c) Downtown Aachen, γ=-101 dBm.

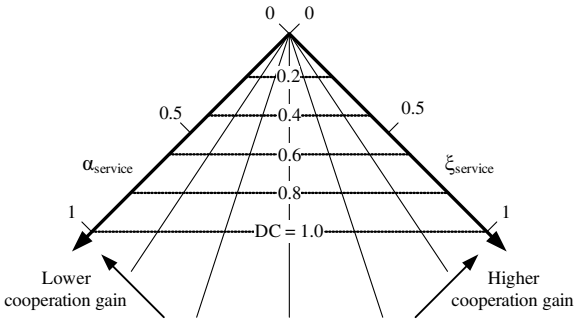

(d) Relation between DC, $\alpha_{service}$ and $\xi_{service}$.

Fig. 3. Probability distribution $p(\alpha_{ISM}, \xi_{ISM})$ as determined from the measurement results gathered for the ISM band (2400–2483.5 MHz). The distances towards the stationary SA are grouped into distance bins. All shown metrics are normalized.

the equations introduced in Section IV-C and subsequent averaging over all locations in one distance bin. At first we focus our discussion on subfigure 3d. It visualizes the relation $DC = \alpha_{service} + \xi_{service}$ and shows that horizontal lines in the subfigures above correspond to situations with constant DC. Additionally, a higher value of $\alpha_{service}$ indicates smaller cooperation gain and a higher value for $\xi_{service}$ describes a scenario with high cooperation gain.

When now focusing on subfigure 3a, it becomes clear that the cooperation gain increases with distance because the higher probability values move from the extreme left further to the right when going from graphs for shorter distances to the ones above for higher distances. This confirms the theoretical findings that cooperative users should be located as far away from each other as possible in order to limit the loss in cooperation gain due to correlated shadowing [20], [30].

When taking into account also subfigure 3b, which is based on a higher detection threshold, we can confirm another theoretical result[17]. As expected, the determined DC-values are lower because the probability of missed detection increases with the higher detection threshold. Additionally, the trend towards higher cooperation gain starts earlier and is more pronounced. As determined by, e.g. Mishra *et al.* in [20], cooperation can help to lower the sensitivity requirements on single sensors because fast fading effects can be compensated. Our results confirm this result in a practical scenario.

Subfigure 3c is computed from the results measured in the downtown area in Aachen using the more sensitive detection threshold. The amount of WLAN-traffic detected throughout this measurement was significantly lower compared to the busy CeBIT industry fair. The low DC reduces the reliability of the gathered results showing that the general applicability of the binary probability metrics is limited by their dependence on the DC.

For the CeBIT hall measurements, Figure 4 shows in more

[17]All detection thresholds applied in this paper were selected in order to keep the noise-triggered false alarm probability at a reasonable level.

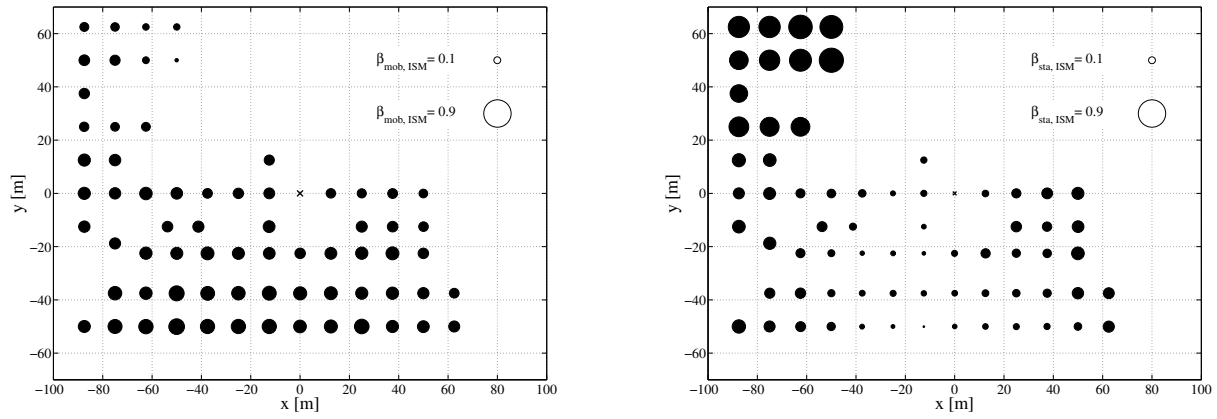

(a) $\beta_{mob,ISM}$.

(b) $\beta_{sta,ISM}$.

Fig. 4. The metrics $\beta_{mob,ISM}$ and $\beta_{sta,ISM}$ as determined from the measurement results gathered for the ISM band (2400–2483.5 MHz) at the CeBIT industry fair. The stationary SA is located at $(x, y) = (0, 0)$ and marked with a cross. Two additional circles without filling were added for value-comparison purposes. The metric $\beta_{mob,ISM}$ gives the amount of new information that the stationary SA can get from the mobile SA and the ratio $\beta_{sta,ISM}$ describes how much new information the stationary SA can provide to the mobile SA. Both metrics are normalized.

detail how the cooperation gain changes over space. The stationary SA was located at $(x, y) = (0, 0)$ and the mobile SA was moved around. All locations at $y \leq 12.5\,\text{m}$ lie in the CeBIT halls 14 and 15, which continues further in the negative y-direction. Locations with $y > 12.5\,\text{m}$ lie in the passage to the hall 16 or the hall 16 itself, which is separated by concrete walls.

The ratio $\beta_{mob,ISM}$ clearly increases when going further away from the stationary SA (Figure 4a). Similarly, also the amount of new information that the mobile SA could receive from the stationary SA increases when the mobile moves further away as indicated by $\beta_{sta,ISM}$ (Figure 4b). The locations in the hall 16 are exceptions. The DC in this area was much lower compared to the halls 14 and 15. Thus, the mobile SA can still benefit from the stationary SA significantly but it does not detect comparable amount of primary user signals and cannot report similar amount of new information back to the stationary SA.

We found similar clusters also in our Aachen campaigns when investigating, e.g., deployed DECT systems. In residential areas higher DC values were measured but around the large Aachen cathedral and the city hall less DECT traffic was detected. CRs will have to take such topology dependence into account when optimizing the sensing process.

B. Correlation metrics

After showing how we could confirm major theoretical results using our practical measurement setup, we will now come back to the goal of enhancing the cooperative sensing process by distributing the sensing task more efficiently. We discussed in Section IV-A and IV-D different metrics to evaluate the similarity of distributed spectrum measurements. We continue by presenting appropriate results that validate our theoretical expectations.

Figure 5 shows that the cross-correlation $R(\mathbf{U}, \mathbf{V})$ is susceptible to differences in the DC. The values computed for the DECT system are higher compared to the ISM-band in the Aachen downtown campaign. However, both other metrics provide very similar values for these technologies. The latter behaviour is more probable because both technologies have a comparable range and consist of multiple privately owned very small networks. Additionally, the cross-correlation also underestimates the drop in similarity over distance for the CeBIT-measurements. Again, the amount of traffic received throughout the halls 14 and 15 was constantly high leading to very high values in the cross-correlation.

In the first examples the normalized covariance $\rho(\mathbf{U}, \mathbf{V})$ showed satisfactory performance. However, Figure 6 is based on the Aachen measurements using a coarser grid and investigates cellular technologies. Especially, the continuously transmitting UMTS downlink (DL) is completely misinterpreted by the normalized covariance $\rho(\mathbf{U}, \mathbf{V})$ as already discussed in Section IV-B.

In contrast, the weighted *AND*/*OR* metric $\Phi_{service}$ successfully describes the similarity behaviour of all different technologies. It is also less dependent on the absolute power levels. This can be seen when comparing the GSM DL and the UMTS DL. In the cross-correlation Figure 6a the GSM DL seems to exhibit higher similarity. However, this is due to the higher transmit power values of the TDMA-based technology compared to the spread spectrum based UMTS system. Since the UMTS signal is continuously transmitted with limited power control adaptations, it should show a higher similarity at least for short distances. Such behaviour is confirmed by the weighted *AND*/*OR* metric $\Phi_{service}$, which outperforms the existing metrics because of its general applicability and its clearly lower dependence on the DC and the absolute received power level.

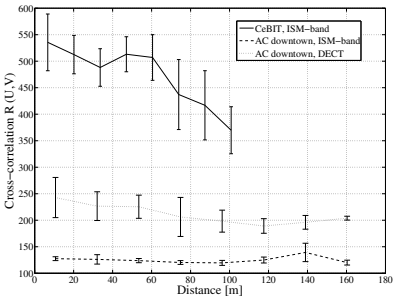

(a) Cross-correlation $R(\mathbf{U}, \mathbf{V})$

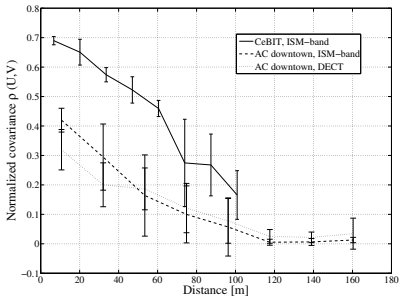

(b) Normalized covariance $\rho(\mathbf{U}, \mathbf{V})$

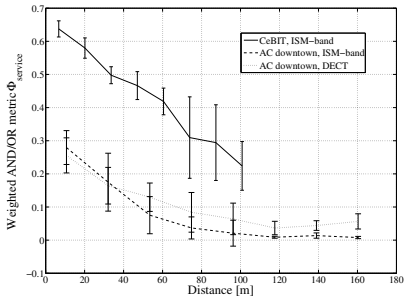

(c) Weighted *AND*/*OR* metric $\Phi_{service}$

Fig. 5. Comparison of the correlation metrics. Each one is averaged over the complete spectrum band and grouped based on the distance to the stationary setup. The errorbars show the standard deviation over the locations in each distance bin. The results are based on the measurements with finer grids.

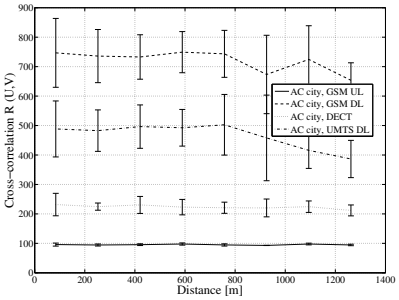

(a) Cross-correlation $R(\mathbf{U}, \mathbf{V})$

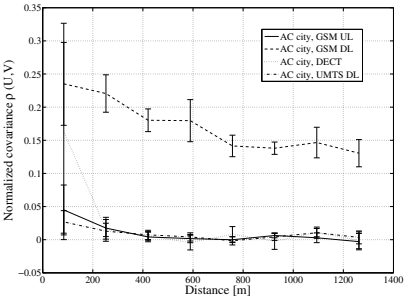

(b) Normalized covariance $\rho(\mathbf{U}, \mathbf{V})$

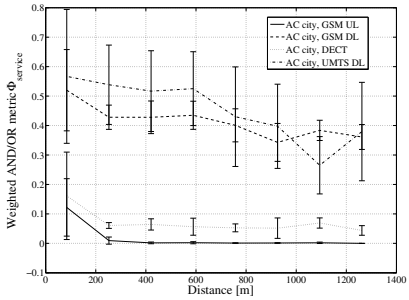

(c) Weighted *AND*/*OR* metric $\Phi_{service}$

Fig. 6. Comparison of the correlation metrics. Each one is averaged over the complete spectrum band and grouped based on the distance to the stationary setup. The errorbars show the standard deviation over the locations in each distance bin. The results are based on the measurements with the coarser grid.

VI. Modelling spectrum

Secondary users could examine the correlation between their spectrum measurements in order to initialize an efficient distribution of the spectrum sensing task over all nodes. We introduced a more robust metric for such correlations and saw that they can be assessed through measurements. However, the initialization phase of such a system is non-trivial and several open problems remain and motivate further research.

First, the standard deviation of the correlations of spectrum measurements is high and increases the required number of measurements to compute sufficient statistics. Second, the impact of mobility or other changes in the environment on the behaviour of these correlations over time is nearly unexplored in the context of DSA networks. Third, the system architecture of DSA networks has significant impact on how the presented results can be further developed to setups with more than two users. Does every user have to evaluate its correlation to any other user in the network or does a single node take care of the correlation analysis and sensing coordination in a centralized fashion?

Fourth, but most prominently, the case with very low duty cycle deserves further investigation. Since only few, if any, primary system transmissions can be detected in this case, sufficient statistics for the correlations can hardly be determined. The fact that two secondary users both do not sense a primary user signal and measure only noise is obviously not sufficient to conclude that their measurements are correlated. However, this case is the most important one in DSA networks because rarely used frequency bands are most valuable to secondary users. In such scenarios, additional information about primary and secondary user locations or further modelling of the environment have to be applied. Another example for such more advanced problems would be collaborative interference minimization as a distributed optimization problem.

In this context, we believe that the construction of probabilistic models of different characteristics of spectrum will be necessary. Such models could either be used directly in CRs to reason about spectrum usage, or as analysis tools in calculations and simulations when carrying out research in the CR/DSA domain. We foresee two major classes of spectrum models [46]. In the first of these, the locations of transceivers are modelled separately, after which traffic and propagation models are used to derive a corresponding model for spectrum. In the second, spectrum is modelled as a *random field*, which is the extension of the usual theory of stochastic processes from one-dimensional *time* to multi-dimensional *space*.

Regarding the first approach, we have studied in earlier work the modelling and characterization of node locations in wireless networks using the stochastic geometry of point processes [47], [48]. In particular, we have shown that it

is possible to create probabilistic models of the location distributions that faithfully represent the second-order statistics of locations and densities of the nodes. The resulting random field from such a modelling process is of the form

$$Z(\mathbf{y}) = \sum_{\mathbf{x}_i \in N} L(\mathbf{x}_i, \mathbf{y}) P_{tx,i}(\theta_{\mathbf{x}_i \to \mathbf{y}}), \tag{18}$$

where $N = \{\mathbf{x}_1, \ldots, \mathbf{x}_n\}$ is the point process model of node locations, L is the model for path loss (either deterministic or stochastic), $P_{tx,i}(\theta)$ is the transmission power of node i into direction θ, and $\theta_{\mathbf{x}_i \to \mathbf{y}}$ is the direction from $\mathbf{x}_i$ to $\mathbf{y}$. We believe this approach to be most applicable to cases where the duty cycle is relatively constant, or when rough estimates on spectral characteristics suffice. Otherwise the precise modelling of the activity of the transmitters will be the major remaining challenge to be solved.

For the second, purely statistical approach to spectrum modelling, we have argued [46] that a straightforward approach to first-principles modelling of spectrum is to consider the *semivariogram*

$$\gamma(\mathbf{x}, \mathbf{y}) \equiv \frac{1}{2} \mathbb{E}\left\{ |Z(\mathbf{x}) - Z(\mathbf{y})|^2 \right\}, \tag{19}$$

where $Z(\mathbf{x})$ is the random variable giving the value of the spectrum characteristic of interest at location $\mathbf{x}$. From experimental data the semivariogram can be estimated by the simple method-of-moments technique, yielding the *empirical semivariogram*

$$\hat{\gamma}(d) \equiv \frac{1}{2|N(d)|} \sum_{N(d)} (Z_j - Z_i)^2, \tag{20}$$

where $N(d)$ denotes the set of pairs (i, j) such that $d - \Delta \leq \|\mathbf{x}_j - \mathbf{x}_i\| \leq d + \Delta$, and $\Delta > 0$ determines the width of the radial bins used. Standard techniques can then be used to fit stochastic models to the empirical variogram. For detailed discussion on these techniques we refer the reader to [46] and references cited therein.

VII. Conclusions

Most work on cooperative sensing has been theoretical in nature. In this paper we presented our specifically developed measurement setup for a detailed evaluation of cooperative sensing in practical scenarios. We enabled autonomous measurements in large scale outdoor environments and provided the required methodology on the way towards practical DSA applications. Via analysis of our extensive measurement results we confirmed major theoretical findings on cooperative sensing, i.e., that cooperation gain increases with the distance between nodes and that cooperation can help to alleviate sensitivity requirements.

Cooperative sensing can be improved by distributing the sensing task across cooperating nodes in order to lower the overall sensing time and power consumption. The same sensing reliability can be maintained because correlations of spectrum measurements over space can be exploited. We have developed a robust metric for evaluating these correlations between spectrum measurements of two secondary users and compared its superior performance to classical correlation metrics. We showed that sufficient statistics can be assessed via measurements. However, it is not clear, yet, if such behaviour definitely requires runtime analysis of the correlations of distributed spectrum measurements or if a similar gain can be achieved by applying precomputed statistical models. Additionally, also the most suitable type or combination of such models is not known. We discussed appropriate candidates that should be explored further.

Finding the borderline between purely statistical modelling and building a system model of the complete radio environment with explicit modelling of transmitter locations and propagation effects will be a part of our future research. In addition, we are currently in the process of restructuring the vast amount of measurement data and will make it available to the community in an appropriate fashion.

Acknowledgment

The authors would like to thank RWTH Aachen University and the German Research Foundation (Deutsche Forschungsgemeinschaft, DFG) for providing financial support through the UMIC excellence cluster. We would also like to thank the European Union for providing partial funding of this work through the ARAGORN project. Additionally, we would like to thank the Deutsche Messe AG for providing us access to our measurement locations at the CeBIT industry fair.

References

[1] Federal Communications Commission, "Spectrum Policy Task Force," Report ET Docket no. 02-135, November 2002.

[2] M. A. McHenry, P. A. Tenhula, D. McCloskey, D. A. Roberson, and C. S. Hood, "Chicago Spectrum Occupancy Measurements & Analysis and a Long-term Studies Proposal," in *Proc. of Workshop on Technology and Policy for Accessing Spectrum (TAPAS)*, Boston, MA, USA, August 2006.

[3] R. I. C. Chiang, G. B. Rowe, and K. W. Sowerby, "A Quantitative Analysis of Spectral Occupancy Measurements for Cognitive Radio," in *Proc. of IEEE Vehicular Technology Conference (VTC)*, Dublin, Ireland, April 2007.

[4] V. Blaschke, H. Jäkel, T. Renk, C. Klöck, and F. K. Jondral, "Occupation measurements supporting dynamic spectrum allocation for cognitive radio design," in *Proc. of International Conference on Cognitive Radio Oriented Wireless Networks and Communications (CROWNCOM)*, Orlando, FL, USA, August 2007.

[5] M. Wellens, J. Wu, and P. Mähönen, "Evaluation of spectrum occupancy in indoor and outdoor scenario in the context of cognitive radio," in *Proc. of International Conference on Cognitive Radio Oriented Wireless Networks and Communications (CROWNCOM)*, Orlando, FL, USA, August 2007.

[6] M. Islam, G. L. Tan, F. Chin, B. E. Toh, Y.-C. Liang, C. Wang, Y. Y. Lai, X. Qing, S. W. Oh, C. L. Koh, and W. Toh, "Spectrum Survey in Singapore: Occupancy Measurements and Analyses," in *Proc. of International Conference on Cognitive Radio Oriented Wireless Networks and Communications (CROWNCOM)*, Singapore, May 2008.

[7] I. F. Akyildiz, W.-Y. Lee, M. C. Vuran, and S. Mohanty, "Next generation/dynamic spectrum access/cognitive radio wireless networks: a survey," *Elsevier Computer Networks Journal*, vol. 50, no. 13, pp. 2127–2159, September 2006.

[8] Q. Zhao and B. Sadler, "A Survey of Dynamic Spectrum Access," *IEEE Signal Processing Magazine*, vol. 24, no. 3, pp. 79–89, 2007.

[9] R. W. Brodersen, A. Wolisz, D. Cabric, S. M. Mishra, and D. Willkomm, "White Paper: CORVUS - A Cognitive Radio Approach for Usage of Virtual Unlicensed Spectrum," University of California, Berkeley, Tech. Rep., 2004, available online http://bwrc.eecs.berkeley.edu/Research/MCMA/CR_White_paper_final1.pdf [Cited on 11th January 2008].

[10] T. Yucek and H. Arslan, "A Survey of Spectrum Sensing Algorithms for Cognitive Radio Applications," *IEEE Communications Surveys & Tutorials*, 2008, in press.

[11] H. Urkowitz, "Energy Detection of Unknown Deterministic Signals," *Proceedings of the IEEE*, vol. 55, no. 4, pp. 523–531, April 1967.

[12] A. E. Leu, K. Steadman, M. McHenry, and J. Bates, "Ultra Sensitive TV Detector Measurements," in *Proc. of IEEE Symposium on New Frontiers in Dynamic Spectrum Access Networks (DySPAN)*, Baltimore, MD, USA, November 2005.

[13] C. Cordeiro, M. Ghosh, D. Cavalcanti, and K. Challapali, "Spectrum Sensing for Dynamic Spectrum Access of TV Bands," in *Proc. of International Conference on Cognitive Radio Oriented Wireless Networks and Communications (CROWNCOM)*, Orlando, FL, USA, August 2007.

[14] W. A. Gardner, "Signal interception: A unifying theoretical framework for feature detection," *IEEE Transactions on Communications*, vol. 36, no. 8, pp. 897–906, August 1988.

[15] A. Tkachenko, D. Cabric, and R. W. Brodersen, "Cyclostationary Feature Detector Experiments using Reconfigurable BEE2," in *Proc. of IEEE Symposium on New Frontiers in Dynamic Spectrum Access Networks (DySPAN)*, Dublin, Ireland, April 2007.

[16] R. Tandra and A. Sahai, "SNR walls for feature detectors," in *Proc. of IEEE Symposium on New Frontiers in Dynamic Spectrum Access Networks (DySPAN)*, Dublin, Ireland, April 2007.

[17] B. Sklar, *Digital Communications: Fundamentals and Applications*, 2nd ed. Upper Saddle River, NJ, USA: Prentice Hall, 2001.

[18] E. Visotsky, S. Kuffner, and R. Peterson, "On Collaborative Detection of TV Transmissions in Support of Dynamic Spectrum Sharing," in *Proc. of IEEE Symposium on New Frontiers in Dynamic Spectrum Access Networks (DySPAN)*, Baltimore, MD, USA, November 2005.

[19] A. Ghasemi and E. S. Sousa, "Collaborative Spectrum Sensing for Opportunistic Access in Fading Environments," in *Proc. of IEEE Symposium on New Frontiers in Dynamic Spectrum Access Networks (DySPAN)*, Baltimore, MD, USA, November 2005.

[20] S. M. Mishra, A. Sahai, and R. W. Brodersen, "Cooperative Sensing among Cognitive Radios," in *Proc. of IEEE International Conference on Communications (ICC)*, Istanbul, Turkey, June 2006.

[21] D. Cabric, A. Tkachenko, and R. W. Brodersen, "Experimental Study of Spectrum Sensing based on Energy Detection and Network Cooperation," in *Proc. of Workshop on Technology and Policy for Accessing Spectrum (TAPAS)*, Boston, MA, USA, August 2006.

[22] ——, "Spectrum sensing measurements of pilot, energy, and collaborative detection," in *Proc. of IEEE Military Communications Conference (MILCOM)*, Washington, DC, USA, October 2006.

[23] M. Gudmundson, "Correlation model for shadow fading in mobile radio systems," *Electronic Letters*, vol. 27, no. 23, pp. 2145–2146, 1991.

[24] J. C. Liberti and T. S. Rappaport, "Statistics of shadowing in indoor radio channels at 900 and 1900 MHz," in *Proc. of IEEE Military Communications Conference (MILCOM)*, vol. 3, San Diego, CA, USA, October 1992, pp. 1066–1070.

[25] T. S. Rappaport, *Wireless communications, principles and practice*, 2nd ed. Prentice Hall, 2002.

[26] F. Graziosi and F. Santucci, "A general correlation model for shadow fading in mobile radio systems," *IEEE Communications Letters*, vol. 6, no. 3, pp. 102–104, March 2002.

[27] I. Forkel, M. Schinnenburg, and M. Ang, "Generation of Two-Dimensional Correlated Shadowing for Mobile Radio Network Simulation," in *Proc. of International Symposium on Wireless Personal Multimedia Communications (WPMC)*, vol. 2, Abano Terme, Italy, September 2004, pp. 314–319.

[28] K. Yamamoto, A. Kusuda, and S. Yoshida, "Impact of Shadowing Correlation on Coverage of Multihop Cellular Systems," in *Proc. of IEEE International Conference on Communications (ICC)*, vol. 10, Istanbul, Turkey, June 2006, pp. 4538–4542.

[29] K. Sawa, E. Kudoh, and F. Adachi, "Impact of shadowing correlation on spectrum efficiency of a power controlled cellular system," *IEICE Transactions on Communications*, vol. 87, no. 7, pp. 1964–1969, July 2004.

[30] A. Ghasemi and E. S. Sousa, "Asymptotic performance of collaborative spectrum sensing under correlated log-normal shadowing," *IEEE Communications Letters*, vol. 11, no. 1, pp. 34–36, January 2007.

[31] A. Taherpour, Y. Norouzi, M. Nasiri-Kenari, A. Jamshidi, and Z. Zeinalpour-Yazdi, "Asymptotically optimum detection of primary user in cognitive radio networks," *IET Communications*, vol. 1, no. 6, pp. 1138–1145, December 2007.

[32] F. E. Visser, G. J. M. Janssen, and P. Pawelczak, "Multinode Spectrum Sensing Based on Energy Detection for Dynamic Spectrum Access," in *Proc. of IEEE Vehicular Technology Conference (VTC)*, Singapore, May 2008, pp. 1394–1398.

[33] C. Alippi and G. Vanini, "A RSSI-based and calibrated centralized localization technique for Wireless Sensor Networks," in *Proc. of IEEE International Conference on Pervasive Computing and Communications (PerCom)*, Pisa, Italy, March 2006, pp. 301–305.

[34] K. Lorincz and M. Welsh, "MoteTrack: A Robust, Decentralized Approach to RF-Based Location Tracking," *Springer Personal and Ubiquitous Computing, Special Issue on Location and Context-Awareness*, vol. 11, no. 6, pp. 489–503, August 2007.

[35] A. M. Ladd, K. E. Bekris, A. Rudys, G. Marceau, L. E. Kavraki, and D. S. Wallach, "Robotics-based location sensing using wireless ethernet," in *Proc. of ACM International Conference on Mobile Computing and Networking (MobiCom)*, Atlanta, Georgia, USA, 2002, pp. 227–238.

[36] B. L. Mark and A. O. Nasif, "Estimation of Interference-Free Transmit Power for Opportunistic Spectrum Access," in *Proc. of IEEE Wireless Communications and Networking Conference (WCNC)*, Las Vegas, NV, USA, April 2008, pp. 1679–1684.

[37] R. Viswanathan and P. K. Varshney, "Distributed Detection with Multiple Sensors: Part I - Fundamentals," *Proceedings of the IEEE*, vol. 85, no. 1, pp. 54–63, January 1997.

[38] R. S. Blum, S. A. Kassam, and H. V. Poor, "Distributed Detection with Multiple Sensors: Part II - Advanced Topics," *Proceedings of the IEEE*, vol. 85, no. 1, pp. 64–79, January 1997.

[39] S. Aldosari and J. Moura, "Saddlepoint approximation for sensor network optimization," in *Proc. of IEEE International Conference on Acoustics, Speech, and Signal Processing (ICASSP)*, vol. 4, March 2005, pp. 741–744.

[40] N. Gnanapandithan and B. Natarajan, "Joint Optimization of Local and Fusion Rules in a Decentralized Sensor Network," *Journal of Communications*, vol. 1, no. 6, pp. 9–17, 2006.

[41] W. Hu, D. Willkomm, M. Abusubaih, J. Gross, G. Vlantis, M. Gerla, and A. Wolisz, "Dynamic Frequency Hopping Communities for Efficient IEEE 802.22 Operation," *IEEE Communications Magazine*, vol. 45, no. 5, pp. 80–87, May 2007.

[42] Rohde & Schwarz, "Spectrum Analyzer R&S FSL Specifications, version 3.00," April 2006.

[43] J. Mitola III, *Cognitive radio: an integrated agent architecture for software defined radio*. Stockholm, Sweden: Ph.D. Thesis, KTH (Royal Institute of Technology), 2000.

[44] Y. Zhao, B. Le, and J. H. Reed, *Cognitive Radio Technology*. Elsevier, 2006, ch. Network Support - The Radio Environment Map, pp. 337–363.

[45] Y. Zhao, L. Morales, J. Gaeddert, K. K. Bae, J.-S. Um, and J. H. Reed, "Applying Radio Environment Maps to Cognitive Wireless Regional Area Networks," in *Proc. of IEEE International Symposium on New Frontiers in Dynamic Spectrum Access Networks (DySPAN)*, Dublin, Ireland, April 2007, pp. 115–118.

[46] J. Riihijärvi, P. Mähönen, M. Wellens, and M. Gordziel, "Characterization and Modelling of Spectrum for Dynamic Spectrum Access with Spatial Statistics and Random Fields," *accepted for publication in Proc. of International Workshop on Cognitive Radios and Networks (CRNETS) in conjunction with IEEE PIMRC*, Cannes, France, September 2008.

[47] J. Riihijärvi, P. Mähönen, and M. Rübsamen, "Characterizing wireless networks by spatial correlations," *IEEE Communications Letters*, vol. 11, no. 1, pp. 37–39, January 2007.

[48] J. Riihijärvi and P. Mähönen, "Exploiting spatial statistics of primary and secondary users towards improved cognitive radio networks," in *Proc. of International Conference on Cognitive Radio Oriented Wireless Networks and Communications (CROWNCOM)*, Singapore, May 2008.